Numerical Model of an Argon Atmospheric Pressure RF Discharge

N. Balcon, G. J. M. Hagelaar, and J. P. Boeuf

***Abstract*—Radio-frequency discharges are known to operate in two different regimes. The α regime of low current density and the γ regime with higher current density. Our recent simulation results suggest that the formation of filaments observed in an atmospheric pressure argon discharge under RF excitation could be triggered by the regime transition $\alpha \rightarrow \gamma$. A unidimensional fluid model taking into account the external circuit shows that above 120 mA/cm^2, the differential conductivity of the discharge becomes negative with a rapid increase in density which can lead to the formation of filaments. As the transition to the γ regime is due to secondary electrons, this threshold value depends on the secondary emission coefficient. In the γ regime, the instantaneous cathode is sustained by secondary electron emission, which drastically changes the behavior of the discharge. In this paper, we present a numerical analysis of the transition between the two regimes and discuss how this could result in the filamentary mode observed in argon RF discharges.**

***Index Terms*—Alpha and gamma regime, atmospheric pressure discharges, fluid model, RF discharges, $\alpha \rightarrow \gamma$ transition.**

I. Introduction

ATMOSPHERIC pressure discharges in various gases have recently received an increasing amount of attention due to their ability to modify the surfaces of polymer films at low cost [1]–[4]. The absence of vacuum systems and pumping down time is very attractive for the plasma processing industry. Open plasma reactors in which samples can be treated in line have also been developed in order to further increase the time efficiency of the surface treatment.

Most of atmospheric pressure discharges are dielectric barrier discharges (DBDs) operating in the kilohertz region. In helium, new sources running at much higher frequencies in the RF range are currently under investigation [5], [6]. These discharges are similar to lower pressure RF discharges with capacitive sheaths. Many authors have pointed out the effect of the transition of RF regime $\alpha \rightarrow \gamma$ on the discharge parameters [7]–[14]. They show that in helium, this transition occurs at atmospheric pressure similarly to a low-pressure RF discharge. The understanding of the mechanisms involved in this transition is of great interest in order to maintain the discharge in a homogeneous state.

In this paper, we will focus on the possibility of using argon instead of helium with the same RF DBD configuration as reported in [15] and [16]. A localized filament is subjected to a large current the associated gas heating can severely damage the polymer film to treat. By limiting the current, the dielectric layer greatly favors the glow mode.

There are very few reports on the $\alpha \rightarrow \gamma$ transition in pure argon. The regime transition has often been described in helium, but its effects on the creation of filaments in argon has not been investigated. In the α mode, the ionization in the sheaths is mainly insured by the oscillating electric field. When the discharge current exceeds a certain value, the production of energetic electrons by secondary emission allows the cathode sheath to be self-sustained. This corresponds to the γ mode of the discharge. The regime transition $\alpha \rightarrow \gamma$ could play a role in the formation of filaments experimentally observed in argon RF DBDs.

II. Description of the Model

A self-consistent unidimensional fluid model has been developed in order to investigate the mechanisms involved in an argon atmospheric RF discharge. The plasma equations are solved in the direction perpendicular to the electrode surface. We use the classical fluid approach which consists in solving the first moments of Boltzmann equation.

A. Governing Equations and Boundary Conditions

The continuity equation is solved for neutral atoms, ions, and electrons

$$\frac{\partial n}{\partial t} + \nabla \cdot \mathbf{\Gamma} = S \tag{1}$$

where n is the particle density, Γ the particle flux, and S is the source term accounting for loss and creation. Using the drift-diffusion approximation, the transport of particles is given by the equation

$$\mathbf{\Gamma} = \pm n\mu\mathbf{E} - D\nabla n \tag{2}$$

where $\mathbf{E}$ is the electric field, μ and D are the mobility and the diffusion coefficient, respectively.

At such high frequency, particular care must be taken when neglecting the ion inertia term $(\partial/\partial t)m_i n_i \overline{\mathbf{v}}$. It is necessary to quantitatively ensure that the ion-neutral collision frequency ν is sufficient for the inertia term to be negligible. In our conditions, the ion mobility is around $\mu_i = 1.6 \times 10^{-4}$ m$^2 \cdot$ V$^{-1} \cdot$ s^{-1} so the collision frequency is approximately $\nu \simeq 1.5 \times 10^{10}$ s^{-1}. This is three orders of magnitude higher than the applied frequency $(13.56 \times 10^6$ s$^{-1})$. Hence, despite

Manuscript received February 9, 2008; revised June 17, 2008. Current version published November 14, 2008.

The authors are with the LAboratoire PLAsma Conversion d'Energie (LAPLACE), 118 Route da Narbonne, 31062 Toulouse, France (e-mail: nicolas.balcon@lea.univ-poitiers.fr).

Digital Object Identifier 10.1109/TPS.2008.2003135

the high frequency the drift-diffusion approximation is still valid.

The equation of energy (3) is solved for electrons

$$\frac{\partial n_\varepsilon}{\partial t} + \nabla \cdot \mathbf{\Gamma}_\varepsilon = H - P(\overline{\varepsilon}) \tag{3}$$

where $n_\varepsilon = \overline{\varepsilon} n_\mathrm{e}$ is the energy density, $\mathbf{\Gamma}_\varepsilon$ is the electron mean energy flux, H is the heating term, $P(\overline{\varepsilon})$ is the energy loss, and $\overline{\varepsilon}$ is the electron mean energy.

In the local field approximation (LFA), it is assumed that there is no transport of energy in the system other than collisional processes. This hypothesis comes down to neglecting the energy flux terms in the electron energy equation (3). In particular, it implies that the energy of electrons is directly linked, spatially and temporally to the electric field, and that their heating is exactly balanced by the energy loss in collisions. This hypothesis can be unsatisfied in the regions of fast electric field variations. If the mean free path of electrons is not small with respect to the characteristic distance of field variations, electrons can gain energy at a particular position and dissipate it somewhere else. In our conditions, the electron mean free path is approximately 1 μm. Therefore, it is more appropriate in our case to solve the equation of energy for the electrons (3). In the case of helium, numerical solutions were found with the LFA, but in the case of argon, the use the equation of energy for electrons was necessary for the model to converge. In this equation, the heating term H is calculated as follows:

$$H = -n_\mathrm{e} e\, \mathbf{E} \cdot \overline{\mathbf{v}}_\mathrm{e} \tag{4}$$

where $\overline{\mathbf{v}}_\mathrm{e}$ is the electron mean velocity.

The energy loss is calculated as follows:

$$P(\overline{\varepsilon}) = -n_\mathrm{e} \overline{\nu}_\mathrm{e} \overline{\varepsilon} \tag{5}$$

where $\overline{\nu}_\mathrm{e}$ is the energy transfer frequency.

The energy flux is calculated as follows:

$$\mathbf{\Gamma}_\varepsilon = -n_\varepsilon \mu_\varepsilon \mathbf{E} + D_\varepsilon \nabla n_\varepsilon \tag{6}$$

where $\mu_\varepsilon = 5/3 \mu_\mathrm{e}$ the energy mobility and $D_\varepsilon = 5/3 D_\mathrm{e}$ its diffusion coefficient.

The electric field is solved in Poison equation

$$\nabla \cdot \mathbf{E} = \frac{1}{\epsilon_0} \sum_s q_s n_s \tag{7}$$

where ϵ_0 is the vacuum permittivity, q_s is the charge of the particle of index s, and n_s is their density.

The boundary conditions are imposed by the particle losses at the walls. The thermal velocity (T_e calculated by the model for electrons and 300 K for ions) gives the particle flux due to thermal motion $n v_\mathrm{t}/4$. These boundary conditions are also applied to the mean electron energy which is treated as a particle of thermal velocity $v_{\mathrm{t},\varepsilon} = (5/3) v_\mathrm{e}$.

Secondary emission of electrons by ion impact on the walls is also taken into account (the secondary emission coefficient is set to 0.1 unless otherwise specified). An electrical model that simulates the circuit behavior when the plasma is turned on is added to the model. As the power supply is not an ideal voltage generator, the potential across the gap drops when a conduction current starts to pass through the discharge. To take this external circuit property into account, a resistor in series with the gap is added after the generator, as shown in Fig. 1. This electrical model is necessary to observe the regime transition $\alpha \rightarrow \gamma$. Without the resistor, the voltage applied to the left electrode would stay constant regardless of the current increase. The existence of the discharge at particular points of the I–V characteristic would not be observed. The simulation is also more stable with this external resistor. Indeed, the breakdown voltage is around 1.4 kV which is too high to simulate the sustain of the plasma.

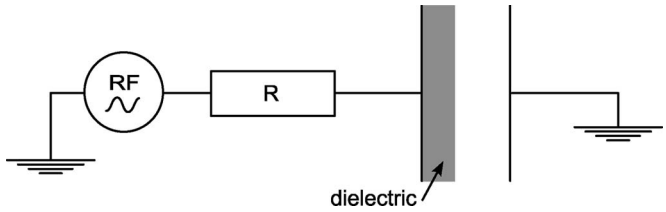

Fig. 1. Electric model of the external circuit.

TABLE I
RATE COEFFICIENTS OF REACTIONS

Reaction	Rate coefficient
$e + Ar \rightarrow 2e + Ar^+$	*BOLSIG+*
$e + Ar \rightarrow e + Ar^\star$	*BOLSIG+*
$e + Ar^\star \rightarrow 2e + Ar^+$	*BOLSIG+*
$2Ar^\star \rightarrow e + Ar^+ + Ar$	$1.2 \times 10^{-9}(300K/T)^{1/2} cm^3 s^{-1}$
$Ar^+ + 2Ar \rightarrow Ar_2^+ + Ar$	$2.5 \times 10^{-31}(300K/T)^{3/2} cm^6 s^{-1}$
$e + Ar_2^+ \rightarrow Ar^\star + Ar$	$7 \times 10^{-7}(300K/T_e)^{1/2} cm^3 s^{-1}$
$Ar^\star \rightarrow Ar + h\nu$	$5 \times 10^5 s^{-1}$
$e + Ar \rightarrow e + Ar$	*BOLSIG+*

B. Numerical Methods and Schemes

As described in [17], the loss term in (5) is linearized with respect to the energy and treated semi-implicitly to prevent numerical instabilities. The flux discretization of charged particles (2) and energy (6) are performed with the exponential scheme as described in [3]. It brings unconditional stability, and it is exact for a constant flux. The coupling between the transport of charged particles and the electric field solved in Poison equation (7) is performed semi-implicitly in order to increase the simulation time step. The transport coefficients and rate coefficients are obtained from the Boltzmann solver BOLSIG+ [18] and from literature [19]–[21].

The model is applied to pure argon with a reduced kinetic scheme containing five species and the seven reactions listed in Table I. In case of argon, it is particularly delicate to take into account excited atoms of the $4s$ system (which contains a resonant and a metastable state). We chose to treat them as a single compound state $Ar^\star$ which groups the resonant and metastable states of argon. Since the energy of metastable and resonant states are very close, there is a large probability for a metastable to turn into a resonant and for a resonant to turn into metastable by electron collisions. Therefore, we assume that they are in Boltzmann equilibrium with the electron

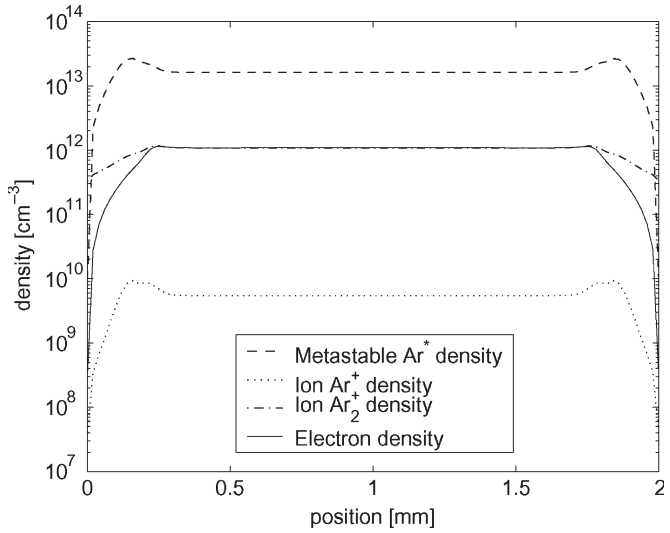

Fig. 2. Particle densities averaged over one RF cycle in the α regime.

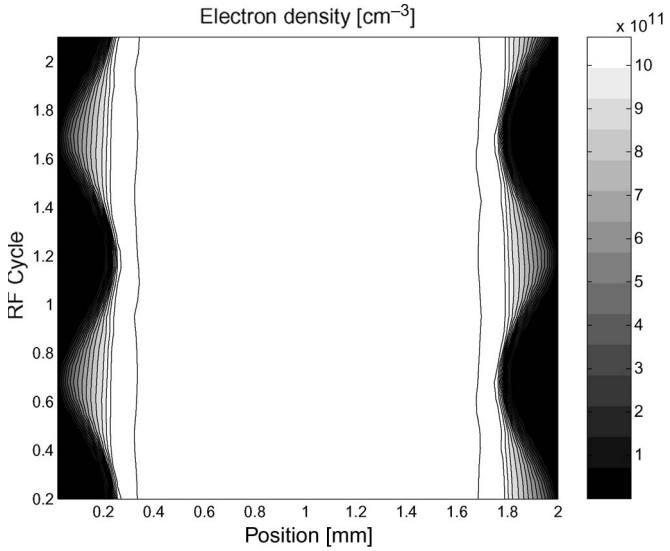

Fig. 3. Electron density evolution in the α regime.

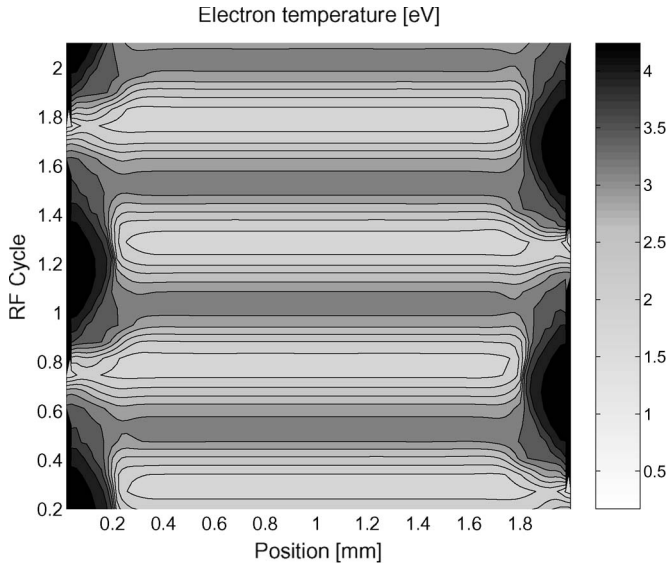

Fig. 4. Electron temperature in the α regime.

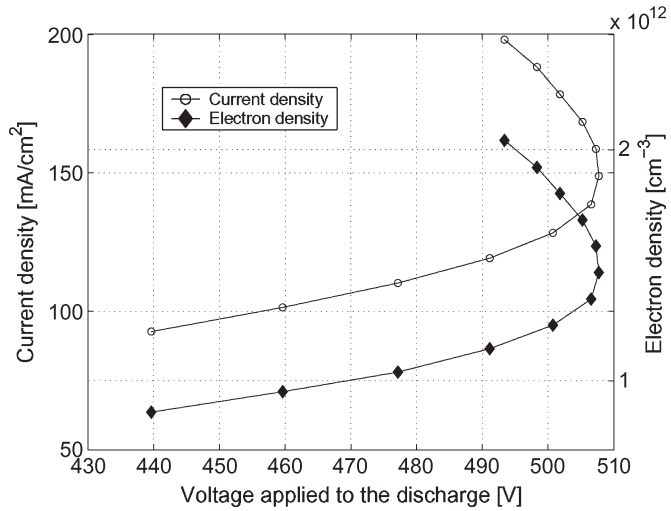

Fig. 5. I–V characteristic (amplitudes of the current and voltage sinelike waveforms) and spatiotemporal average of the electron density.

temperature, and we assign to the compound state an average decay frequency accounting for radiation trapping.

III. Transition α–γ

The simulation results for a discharge gap of 2 mm are presented in this section. The averaged particle densities in the α regime (Fig. 2) show that this discharge is similar to a lower pressure RF capacitive discharge. The particles densities averaged over one RF cycle are constant in the middle of the gap. Similar density profiles are obtained in the γ regime. As seen in Fig. 3, the electron density is constant in the plasma and is strongly modulated in the sheaths. Other species density are constant in the sheaths. This behavior is common to the α and γ regimes.

The results also show that the dominant ions are the dimmers Ar_2^+ as expected at this high pressure. As previously reported for atmospheric argon discharges [22], [23], the metastable atoms population is large and plays an important role in the ionization processes.

The space and time variations of the electron temperature in the α regime are shown in Fig. 4. The electron temperature in the γ regime is of the same order. The temperature in the middle of the gap is around 2.5 eV which is in good agreement with experimental results obtained in the same conditions [24].

The relation between the discharge current and voltage is studied for values up to 180 mA/cm^2. Recent simulation results obtained in pure helium [25] show that the regime transition $\alpha \rightarrow \gamma$ occurs for current density amplitude around 56 mA/cm^2. In the same configuration, in pure argon, the transition occurs at a much higher value of the current density amplitude ($\sim$120 mA/cm^2). The I–V characteristic of Fig. 5 shows the evolution of the voltage amplitude and electron density as a function of the current amplitude. Two main regions of different conductivities are visible.

The slope of the I–V characteristic, i.e., the differential conductivity changes its sign when the current density reaches $\sim$120 mA/cm^2. Each region corresponds to a regime in which the discharge can operate. This characteristic is obtained by increasing the RF voltage applied to the entire discharge circuit composed of the serial resistor and serial dielectric layer (Fig. 1).

In the first part of the I–V characteristic, for values of the current density lower than 120 mA/cm^2, the current linearly increases with a rising voltage as in classical RF discharges. The differential conductivity of the plasma is positive and fairly constant. This behavior is typical of a normal radio-frequency α regime [26], [27].

When the current density reaches 120 mA/cm^2, the voltage is maximum, at 507 V, and the differential conductivity becomes negative. This corresponds to the beginning of the γ regime of the discharge. There are no simulation results for current densities above 180 mA/cm^2 as the validity of the fluid model is questionable in those conditions.

For certain values of the discharge voltage, the two different plasma regimes are possible. For instance, at 500 V, the plasma can exist with an electron density of 1.2×10^{12} cm^{-3} and a current density of 128 mA/cm^2 or with a higher electron density of 1.85×10^{12} cm^{-3} and current density of 180 mA/cm^2.

The electron density, also plotted as a function of the voltage amplitude in Fig. 5, follows a curve similar to the current density. It increases piratically linearly with the voltage amplitude for values below 1.2×10^{12} cm^{-3} and rapidly increases for higher values in the transition region. In the γ regime region of negative differential conductivity, the electron density increases as the voltage decreases.

This transition from the α regime to the γ regime has first been observed experimentally [28] and analyzed with fluid models [29] for low-pressure conditions. It is due to the important production of electrons in the sheath region for large current densities. When the electronic multiplication of the avalanches generated by secondary electrons becomes sufficient, the sheath becomes self-sustained as in a dc discharge. As the ion density rises in the sheaths, the sheath voltage due to the excess of positive space charge rises as well and eventually reaches a threshold value sufficient to sustain the discharge. After the transition to the γ regime, the initial thick ionic layer in the sheath region becomes a normal cathode layer as in the initiation of a normal dc discharge. The sheath region of positive space charge contracts to an optimal value for self-sustainment. The neutral plasma column acts as the anode of a classical dc discharge. The electric field is redistributed in the cathode sheath so that the ionization is more efficient. This behavior is similar to the subnormal regime of dc discharge in which the differential conductivity is negative. The voltage necessary for the self-sustain is smaller than for the nonself-sustained discharge. The present model is limited to current densities lower than 200 mA/cm^2, but we expect that a region of positive differential conductivity will be reached for higher current densities ($\sim$20 A/cm^2) in the filamentary mode as reported experimentally in [30].

The different mechanisms of electron production are shown in Fig. 6(a) for the α regime and Fig. 6(b) for the γ regime. In

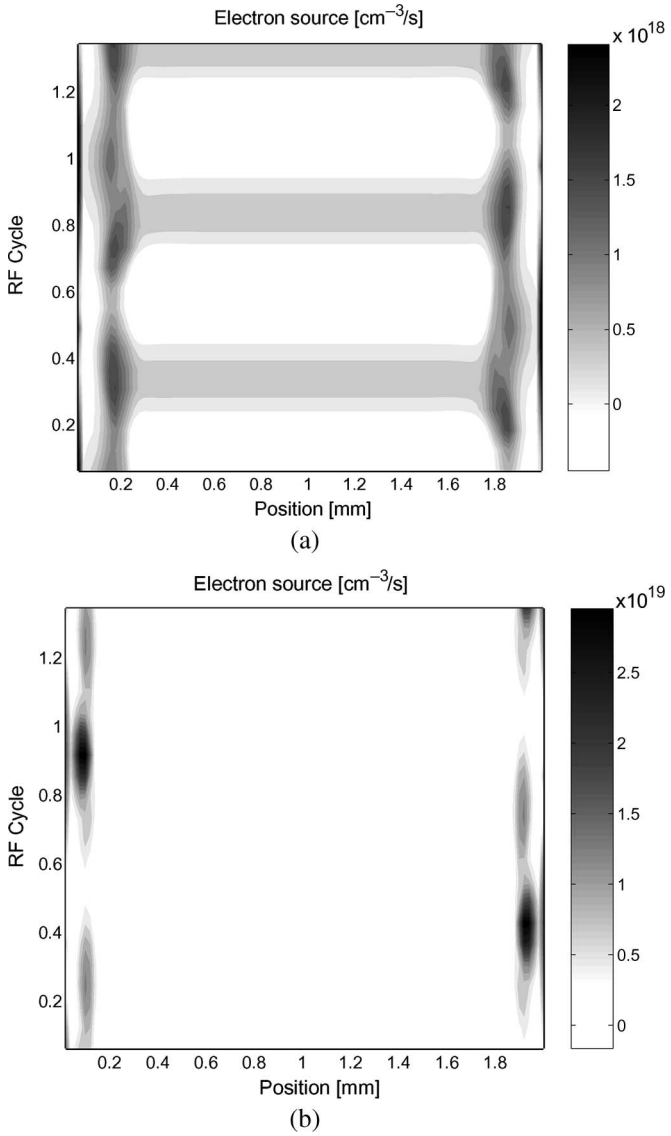

Fig. 6. Electron source in the (a) α regime for a current density of 120 mA/cm^2 and in the (b) γ regime for a current density of 180 mA/cm^2.

the α regime, the electrons created in the sheath (approximately 0.2 mm wide) by the oscillating electric field are not sufficient to sustain it. Electron production by ionization in the sheaths region occurs during the whole RF cycle, and with a larger intensity during sheath expansion, as shown in Fig. 6(a). In the γ regime, the generation in the sheaths is much more important (by one order of magnitude) and occurs mainly at the instantaneous cathode as in a classical dc discharge. The sheath region in this regime is sustained by secondary electrons ("γ electrons," hence the name "γ regime"). In the γ regime, the contribution of secondary emission to the total electron creation is $\sim$17%, whereas it is only $\sim$3% in the α regime.

In the γ mode, the sheath region shrinks, and the averaged plasma potential decreases (because the discharge voltage decreases). The shrink of the sheath results in an increase of the electric field in this region. In Fig. 7, the electron density profiles exhibit the sheath contraction when the current and the electron density rise.

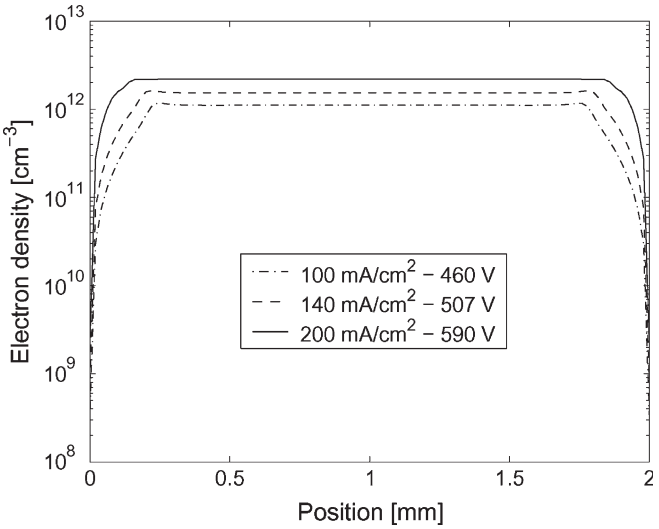

Fig. 7. Density profiles for different regions of the I–V characteristic.

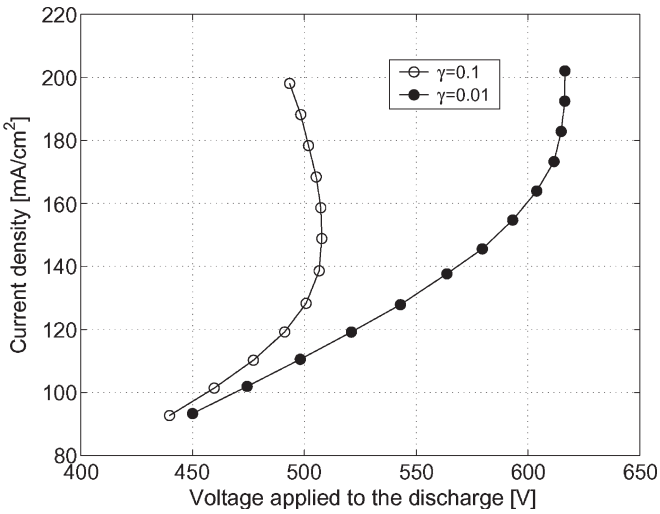

Fig. 8. I–V characteristic for different value of the secondary emission coefficient.

The influence of the secondary emission coefficient on the I–V characteristic is shown in Fig. 8. Its value strongly affects the transition between the two regimes. With a low secondary emission ($\gamma = 0.01$), the α regime can be sustained for higher current densities. At 150 mA/cm^2, the discharge is still in an α regime when the secondary emission coefficient is 0.01, but for a higher secondary emission coefficient of 0.1, the transition to the γ regime already starts. With a greater secondary emission coefficient, the transition $\alpha \rightarrow \gamma$ with sheath contractions occurs for lower values of the current density.

For the same current density of 200 mA/cm^2, the electron density profiles obtained with $\gamma = 0.1$ and $\gamma = 0.01$ are shown in Fig. 9. On each profile, the electron density in the bulk of the plasma is approximately 2×10^{12} cm^{-3} but the sheaths size is smaller with a larger secondary emission coefficient when the discharge is in the γ regime.

The glow mode experimentally observed [24] corresponds to the normal α regime of the discharge. The experimentally measured current densities for the glow mode is around 100 mA/cm^2 with an electron density of 5×10^{11} cm^{-3} which

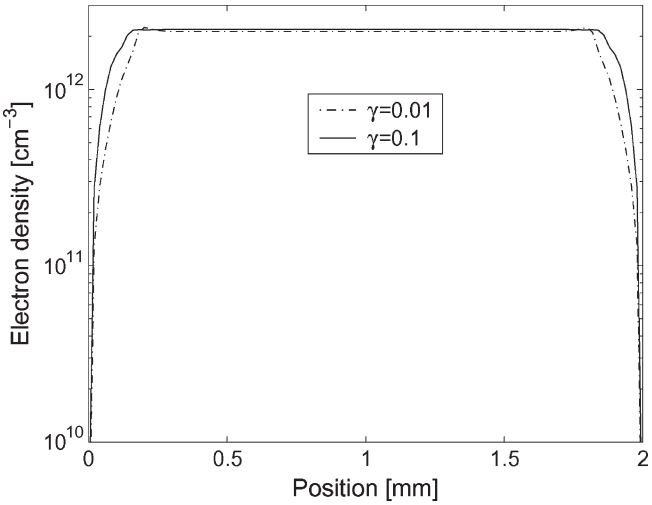

Fig. 9. Electron density for two values of the secondary emission coefficient. Current density = 200 mA/cm^2.

corresponds to the simulation results of the α regime. The total current experimentally measured for the filamentary mode is similar to the glow mode current (identical peak value) but filaments cover a much smaller area of the electrode surface. Hence, the current density in filaments is estimated to be around 20 A/cm^2, and the electron density is measured from Stark broadening to be approximately 10^{15} cm^{-3} [24].

These values are much greater than the current and density values found for the α and γ regimes of the simulation. However, the regime transition $\alpha \rightarrow \gamma$ obtained with the fluid model is possibly responsible for the ignition of the filamentary discharge. The γ part of the I–V curve having a negative differential conductivity makes the discharge electrically unstable. The sudden increase of the plasma density due to the regime transition could also trigger the filament formation in 3-D. If the current density increases up to several amperes per square centimeter, the filamentary mode of much greater density (10^{15} cm^{-3}) can be reached. In this, the filamentary mode the differential conductivity becomes positive again [30] which makes the discharge electrically more stable.

IV. Conclusion

A unidimensional fluid model was used to investigate the transition $\alpha \rightarrow \gamma$ occurring in an atmospheric argon RF discharge. This transition has already been observed both experimentally and numerically in the case of helium but not of argon. As for helium, in the γ regime, the discharge is sustained in the sheath by electrons emitted by the cathode avalanching. However, in argon, the $\alpha \rightarrow \gamma$ transition occurs for current densities higher than in helium (around 120 mA/cm^2 instead of 56 mA/cm^2 for helium). We have only described in this paper the onset of the γ regime, where the sheath becomes self-sustained and the I–V characteristics presents a negative slope, as in the subnormal regime of a dc glow discharge. In this regime, the sheath is still collisional, and its length is much larger than the electron mean free path (and our fluid model with a simple energy equation is valid).

The I–V characteristic of the γ regime with negative differential conductivity and rapid increase of the plasma density corresponds to an unstable state of the discharge. The discharge has a tendency to evolve into another state which can be found in the filamentary mode of much greater density. Although the fluid model does not account for the complex 3-D effects occurring in the gas gap, the $\alpha \rightarrow \gamma$ regime transition observed in simulations could play a role in the formation of filaments experimentally witnessed.

Further work is needed to better understand the formation of filaments at higher current densities in the experiments [24], and to confirm the role of the negative differential conductivity of the discharge in the transition to this regime.

REFERENCES

[1] F. Massines, R. Messaoudi, and C. Mayoux, "Comparison between air filamentary and helium glow dielectric barrier discharges for the polypropylene surface treatment," *Plasmas Polym.*, vol. 3, no. 1, pp. 43–59, Mar. 1998.

[2] J. R. Roth, J. Rahel, X. Dai, and D. M. Sherman, "The physics and phenomenology of one atmosphere uniform glow discharge plasma (OAUGDP) reactors for surface treatment applications," *J. Phys. D, Appl. Phys.*, vol. 38, no. 4, pp. 555–567, Feb. 2005.

[3] M. J. Shenton and G. C. Stevens, "Surface modification of polymer surfaces: Atmospheric plasma versus vacuum plasma treatments," *J. Phys. D, Appl. Phys.*, vol. 34, no. 18, pp. 2761–2768, Sep. 2001.

[4] M. Síra, D. Trunec, P. Stahel, V. Bursíková, Z. Navrátil, and J. Bursík, "Surface modification of polyethylene and polypropylene in atmospheric pressure glow discharge," *J. Phys. D, Appl. Phys.*, vol. 38, no. 4, pp. 621–627, 2005.

[5] S. Y. Moon, W. Choe, and B. K. Kang, "A uniform glow discharge plasma source at atmospheric pressure," *Appl. Phys. Lett.*, vol. 84, no. 2, p. 188, Jan. 2003.

[6] S. Y. Moon, J. K. Rhee, D. B. Kim, and W. Choe, "α, γ, and normal, abnormal glow discharge modes in radio-frequency capacitively coupled discharges at atmospheric pressure," *Phys. Plasmas*, vol. 13, no. 3, p. 033 502, Mar. 2006.

[7] A. S. Smirnov and L. D. Tsendin, "The space-time-averaging procedure and modeling of the RF discharge," *IEEE Trans. Plasma Sci.*, vol. 19, no. 2, pp. 130–140, Apr. 1991.

[8] X. Yang, "Comparison of an atmospheric pressure, radio-frequency discharge operating in the α and γ modes," *Plasma Sources Sci. Technol.*, vol. 14, no. 2, pp. 314–320, May 2005.

[9] J. J. Shi and M. G. Kong, "Mechanisms of the α and γ modes in radio-frequency atmospheric glow discharges," *J. Appl. Phys.*, vol. 97, no. 2, p. 023 306, Dec. 2004.

[10] J. J. Shi, "Sheath dynamics in radio-frequency atmospheric glow discharges," *IEEE Trans. Plasma Sci.*, vol. 33, no. 2, pp. 278–279, Apr. 2005.

[11] J. J. Shi, D. W. Liu, and M. G. Kong, "Plasma stability control using dielectric barriers in radio-frequency atmospheric pressure glow discharges," *Appl. Phys. Lett.*, vol. 89, no. 8, p. 081 502, Aug. 2006.

[12] J. J. Shi, D. W. Liu, and M. G. Kong, "Mitigating plasma constriction using dielectric barriers in radio-frequency atmospheric pressure glow discharges," *Appl. Phys. Lett.*, vol. 90, no. 3, p. 031 505, Jan. 2007.

[13] J. Park, I. Henins, H. W. Herrmann, G. S. Selwyn, and R. F. Hicks, "Discharge phenomena of an atmospheric pressure radio-frequency capacitive plasma source," *J. Appl. Phys.*, vol. 89, no. 1, pp. 20–28, Jan. 2001.

[14] J. Park, "Gas breakdown in an atmospheric pressure radio-frequency capacitive plasma source," *J. Appl. Phys.*, vol. 89, no. 1, p. 15, Jan. 2001.

[15] J. Park, I. Henins, H. W. Herrmann, G. S. Selwyn, J. Y. Jeong, R. F. Hicks, D. Shim, and C. S. Chang, "An atmospheric pressure plasma source," *Appl. Phys. Lett.*, vol. 76, no. 3, p. 288, Jan. 2000.

[16] S. Y. Moon, "Study on discharge modes and characteristics of large-area plasma produced at atmospheric pressure," Ph.D. dissertation, KAIST, Daedeok Sci. Town, South Korea, 2006.

[17] G. Hagelaar, "Modelling of microdischarges for display technology," Ph.D. dissertation, Technische Universiteit Eindhoven, Eindhoven, The Netherlands, 2000.

[18] G. J. M. Hagelaar and L. C. Pitchford, "Solving the Boltzmann equation to obtain electron transport coefficients and rate coefficients for fluid models," *Plasma Sources Sci. Technol.*, vol. 14, no. 4, pp. 722–733, Nov. 2005.

[19] E. V. Karoulina and Y. A. Lebedev, "Computer simulation of microwave and DC plasmas: Comparative characterization of plasmas," *J. Phys. D, Appl. Phys.*, vol. 25, no. 3, pp. 401–412, Mar. 1992.

[20] S. K. Lam, C.-E. Zheng, D. Lo, A. Dem'yanov, and A. P. Napartovich, "Kinetics of Ar_2^+ in high-pressure pure argon," *J. Phys. D, Appl. Phys.*, vol. 33, no. 3, pp. 242–251, Feb. 2000.

[21] B. Min, S. H. Lee, and H. G. Park, "New combination of a three-component gas, Ne–Xe–Ar, for a high efficiency plasma display panel," *J. Vac. Sci. Technol., A, Vac. Surf. Films*, vol. 18, no. 2, pp. 349–355, Mar. 2000.

[22] C. Penache, M. Miclea, A. Bräuning-Demian, O. Hohn, S. Schössler, T. Jahnke, K. Niemax, and H. Schmidt-Böcking, "Characterization of a high-pressure microdischarge using diode laser atomic absorption spectroscopy," *Plasma Sources Sci. Technol.*, vol. 11, no. 4, pp. 476–483, Oct. 2002.

[23] M. C. Penache, "Study of high pressure glow discharges generated by Micro Structured Electrode (MSE) arrays," Ph.D. dissertation, Johann Wolfgang Goethe-Universität, Frankfurt, Germany, 2002.

[24] N. Balcon, A. Aanesland, and R. W. Boswell, "Pulsed RF discharges, glow and filamentary mode at atmospheric pressure in argon," *Plasma Sources Sci. Technol.*, vol. 16, no. 2, pp. 217–225, Jan. 2007.

[25] J. J. Shi and M. G. Kong, "Mode characteristics of radio-frequency atmospheric glow discharges," *IEEE Trans. Plasma Sci.*, vol. 33, pt. 2, no. 2, pp. 624–630, Apr. 2005.

[26] E. E. Kunhardt, "Generation of large-volume, atmospheric-pressure, nonequilibrium plasmas," *IEEE Trans. Plasma Sci.*, vol. 28, no. 1, pp. 189–200, Feb. 2000.

[27] Y. P. Raizer, M. N. Shneider, and N. A. Yatsenko, *Radio-Frequency Capacitive Discharges*. Boca Raton, FL: CRC Press, 1995.

[28] S. M. Levitskii, "An investigation of the breakdown potential of a high-frequency plasma in the frequency and pressure transition regions," *Zhurnal Tekhnicheskoi Fiziki*, vol. 27, p. 970, 1957.

[29] P. Belenguer and J. P. Boeuf, "Transition between different regimes of RF glow discharges," *Phys. Rev. A, Gen. Phys.*, vol. 41, no. 8, pp. 4447–4459, Apr. 1990.

[30] W. T. Sun, G. Li, H. P. Li, C. Y. Bao, H. B. Wang, S. Zeng, X. Gao, and H. Y. Luo, "Characteristics of atmospheric-pressure, radio-frequency glow discharges operated with argon added ethanol," *J. Appl. Phys.*, vol. 101, no. 12, p. 123 302, Jun. 2007.

N. Balcon, photograph and biography not available at the time of publication.

G. J. M. Hagelaar, photograph and biography not available at the time of publication.

J. P. Boeuf, photograph and biography not available at the time of publication.